# High-Speed Radiography Using Laser-Produced X-Rays; Characteristics and Applications

Diploma paper
by
Lars-Johan Hardell

Lund Reports on Atomic Physics, LRAP-217
Lund, July 1997

## Abstract

X-rays from a laser-produced plasma, generated using 100 fs pulses from the table-top terawatt-laser ($T^3$-laser) in Lund, were used for high-speed radiography. The X-ray source is characterised by its short pulse duration, of the order of picoseconds, and the small source size, down to 30 μm. This makes the radiation suitable for high-speed magnification radiography, which is investigated here. A set-up for high-speed imaging using a visible laser pulse as flash is described. The laser based X-ray source is introduced together with an example of high-speed radiography through the imaging of air-gun bullets passing through a phantom. The possibility to use high-speed radiography with a laser based X-ray source in the imaging of a laser ablation phenomenon on the nanosecond scale is discussed, and successfully executed using a high-speed magnification radiography technique.

# Table of contents

# 1. Introduction

High-speed photography is a field that has fascinated many through the years, much thanks to pioneers like Harold E. “Doc” Edgerton at MIT [1] with his famous pictures of water-drops hitting a liquid surface and bullets passing through apples among others. The ability to freeze a short instant of time and make it live forever in a picture reveals details and beauty normally denied the human eye. For some it is a hobby, depicting water-drops splashing into a liquid surface, imaging a bullet passing through an apple, or freezing a bee or bird in flight, but it can also be used for more serious purposes as for example evaluation of ammunition tests [ 2] or study of shock waves [ 3].

The purpose of high-speed photography is to record a fast-moving event. There are a number of different techniques available, and it depends on the event which one is the most suitable. All techniques are based on the same principle - to expose the film (or equivalent, like image plate or CCD-array) to the radiation only for an very short time. This can be done in two separate ways, either by using some kind of high-speed flash in a relatively dark room, leaving the shutter of the camera open, or by using some kind of ultrafast shutter. Electro-optical shutters, based on the Kerr cell, are available for as short exposure times as 5 ns [4], and flashes can be constructed (by adding capacitors and control circuits to a normal photographic flash) with a duration of the order of microseconds (at photographically practical intensities). Flashes exist, however, with a pulse duration as short as about 30 ns [5]. Alternatively, a pulsed laser can be used, delivering high-energetic flashes in a narrow spectral band.

When a motion is imaged, it is often suitable to use some kind of stroboscopic imaging, i.e. using a flash with a high repetition rate, so that the images contain information of how the object looked at several different instants. This is often important when the event is not completely repeatable, when it looks a little bit different from time to time. Otherwise, if the event is repeatable, a possibility is to repeat the event a number of times and take the actual picture at several different delays after the initiation of the event. An example of stroboscopic imaging using laser illumination is given in [6]. Stroboscopic imaging will not be treated in this work since all experiments in this work has been done using lasers with 10 Hz repetition frequency, which is too low for stroboscopic imaging. The events studied here are all partially or completely repeatable.

A common problem in the world of high-speed photography is the triggering, often the photographer wants to decide the exact instant when the picture is made. Here there are also two different approaches, either to trigger the event itself to know exactly when it started, or to detect the event occurring, a few moments before the actual exposure will take place. This detection can be arranged in a number of different ways, for example if the phenomenon is self-luminous a photo-electric trigger could be suitable (to control a shutter) or if the event is initiated with a sound, a microphone could be used. The microphone arrangement can be very elegant, a delay can be introduced simply by moving the microphone away from the source.

Of course, a series of other complications can occur, for example if the object is self-luminous or invisible to the naked eye (like a shock wave or an object moving in an opaque material), that call for more sophisticated imaging methods. If the phenomenon is self-luminous one solution (apart from using the emitted radiation and a fast shutter, not always suitable) is to use a ”flash” of a different wavelength than emitted from the

object, and then filtering the radiation before it reaches the sensitive film (or equivalent). This can often be accomplished by using X-rays when the object emits visible radiation. There is also a rather different approach using the fact that lasers emit very intense radiation in a narrow spectral band. By illuminating the object with a laser pulse with short duration, and filtering the light incident on the film, letting only the laser wavelength pass, luminous objects can be imaged. This can be used, for example, to evaluate ammunition tests [2]. If the object is invisible to the naked eye (or film to be precise), some special property has to be found that can make the event visible to the imaging system. A good example of how the imaging of the invisible can be made is the Schlieren photography technique [3,7], used to photograph shock-waves. It is based on the fact that the index of refraction is dependant on the pressure. In a shock-wave a pressure gradient is formed, and subsequently a gradient in the index of refraction. This gradient will bend the incident light, and this bending of light can be caught on an image. When dealing with a fast event in a material opaque at optical wavelengths the most obvious solution is to use another part of the spectrum for the imaging, where the material is transparent. This would most often be in the X-ray region.

The most common way to generate X-rays is through accelerating electrons in an electric field into a target consisting of a material of some high atomic number. The electrons will collide with the particles in the target, emitting Bremsstrahlung. This technique is employed in X-ray tubes. High-speed X-ray-tubes are available with pulse durations in the sub-microsecond region. Another way to produce X-rays is in synchrotrons. In this work the use of X-rays from a Laser Produced Plasma (LPP) will be discussed for the imaging of a laser ablation process, a strongly luminous event.

The laser-produced plasma X-ray generation is based on the fact that when a high-power laser pulse is focused into a solid target, a plasma is formed, and this plasma emits radiation in a huge spectrum, including X-rays up to the hard-X-ray regime (>100 keV). The LPP X-ray source has some properties that can be desirable for high-speed radiography, above all the short duration of the X-ray pulses, in these experiments of the order of 1 ps, but also the fact that the source is very small can be an advantage, allowing magnification radiography. The plasma also emits a relatively large fraction of characteristic X-rays of the target material. By changing the target material the spectrum of the emitted X-rays can be changed, which can also be of great importance. Today this possibility is used for differential imaging. The short duration of the X-ray pulses, in combination with a gateable detector, allows time-gated viewing. Laser produced X-rays have also been used to study the propagation of laser driven shocks in low density foam targets [8]. The compression of the material in the shocked region then increases the X-ray absorption, making the wave detectable.

The present work contains some different aspects of high-speed imaging, all involving lasers. First, in the next chapter, conventional, laser-based high-speed photography is discussed, and demonstrated, using a rather simple, straight-forward technique. Some short-comings of this technique will be pointed out. After that introductory experiment, the laser produced plasma X-ray source is introduced together with the new possibilities that are opened by using LPP X-rays in high-speed radiography, in chapter 3. Chapter 4 addresses the possibility to use laser produced X-rays for imaging of a laser ablation process. The future possibilities and suggested improvements are discussed in chapter 5

together with applications where high-speed radiography can become an important tool for the imaging and understanding of  our surrounding world.

The aim of this work is to investigate the possibilities to use a Laser Produced Plasma X-ray source in high-speed radiography and especially in one application; the study of laser ablation in an opaque target. The formation of a crater in a target when a nanosecond laser is focused on its surface is an application where the strong visible light and high velocities make the imaging difficult, especially if a profile of the growing crater is desired. This puts some very special constrains on the imaging technique.

# 2. Conventional high-speed photography; A demonstration using visible laser illumination

High-speed photography is normally accomplished through exposing a film (or equivalent) for only a short instant of time, how short exposure time that is required of course depends on the speed of the event that is imaged. Short exposure times can be reached through the use of high-speed flashes or high-speed shutters. In this chapter a demonstration of high-speed photography using a pulsed laser as a flash is described. First the set-up, and then the results achieved will be presented, with a brief discussion of applications and short-comings of this relatively simple technique.

## 2.1 Experimental Set-up

A frequency doubled Nd:YAG-laser (Surelite from Continuum, 532 nm) was used, in principle like an ordinary flash with a pulse duration of approximately 5-7 nanoseconds. In the experiments an air-gun (Haenel, model 310, 4.4 mm calibre) was used to provide the fast objects for the high-speed images. The velocity of the bullets was about 135 m/s. An optical interrupter was placed in front of the air-gun barrel, and was connected to the trigger input of a delay/pulse generator (Model DG535, Stanford Research Systems Inc.). The delay unit outputs were connected to the trigger input ports of the CCD-camera (Star 1, Photometrics Ltd.) and the laser. The use of a CCD-camera for the imaging was favourable because of the fast readout of the pictures. The images were stored as computer files, thus easy to handle. The set-up is shown in Figure 2.1.

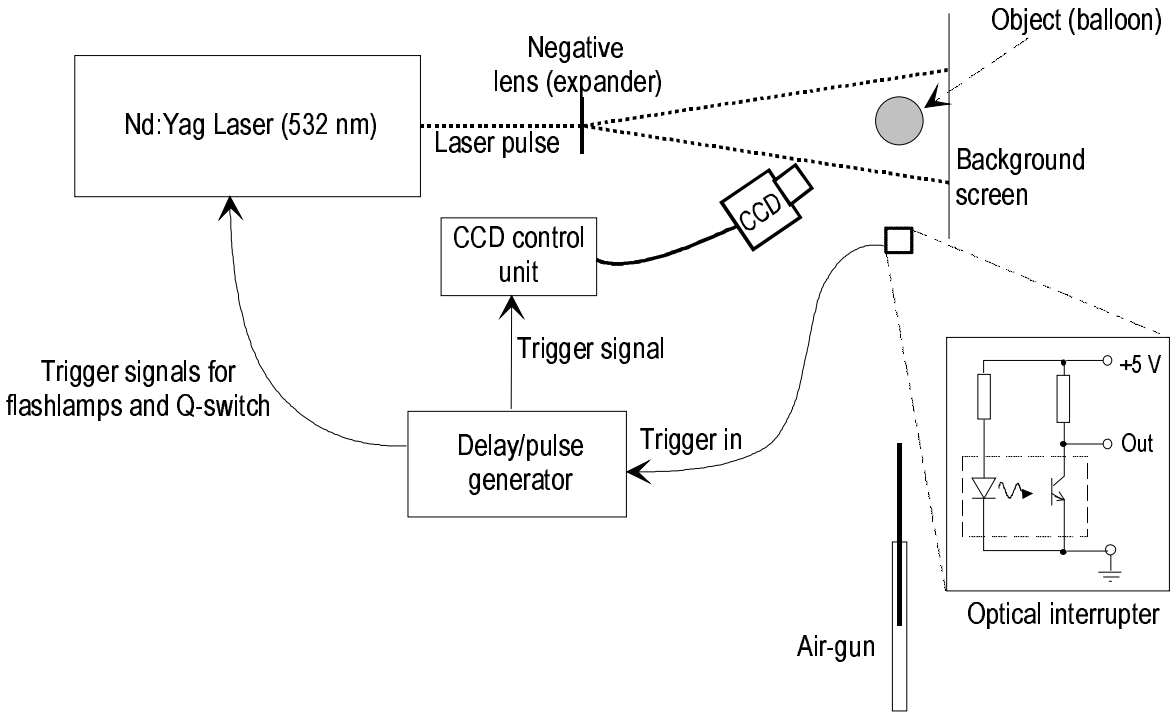


**Figure 2.1.** *The set-up for conventional high-speed imaging using a laser "flash".*

As the air-gun was fired, the interrupter detected the bullet passing by, generating a trigger signal to the delay unit. After the required delay time trigger signals were sent into the laser and the CCD-camera. The CCD-unit was already in trigger position with an open shutter, but continuously clearing the memory until the trigger signal was

registered, then the clearing ceased within 20 microseconds, thus recording an image. Simultaneously a signal was given to the laser flash-lamps, commanding flash, and about 180 microseconds later the laser fire command was given and the laser pulse, expanded in a negative lens, lit up the object during about 7 nanoseconds time. Since the CCD-camera does not have shorter exposure times than 0.1 seconds, the firing had to take place in a rather dark room, but thanks to the laser intensity complete darkness was not required.

## 2.2 Results

Using the set-up described above a number of pictures were taken. The first (and least complicated) pictures were taken without the air-gun, and show a small computer fan (diameter about 4 cm), actually rotating with about 100 revolutions per second, but apparently standing still in the images. For comparison an exposure was made without the laser pulse, using only continuous white light for illumination during the 0.1 s long exposure, resulting, of course, in a blurry image due to the motion of the fan. The images are shown in Figure 2.2. Using the fan as object the trigger problem could be avoided.

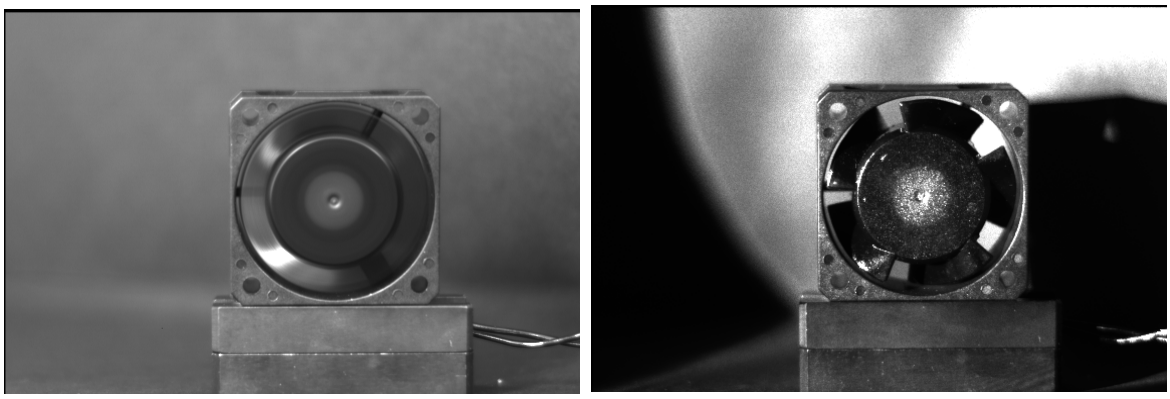

**Figure 2.2** *A small computer fan, both images with the fan rotating with about 100 revolutions per second. The left image is made with continuous white light during the 0.1 seconds exposure time, the right image shows the high-speed picture using the laser "flash".*

The next pictures were made using an air-gun in the set-up described above, shooting at small balloons. Now the timing was more crucial, so a sensor was used to detect the bullet, as described in the previous section. By adjusting the delay time on the delay/pulse generator it could be decided with a rather good accuracy how far the bullet should have reached when the image was made, using the fact that the speed of the bullets were known to be 135 m/s (not measured in these experiments). A series of pictures were taken, showing in detail how the balloon is stretched and deformed before it actually bursts, a phenomenon to fast to see with the human eye, but made visible through this technique. Some of the resulting images are shown in Figure 2.3 below.

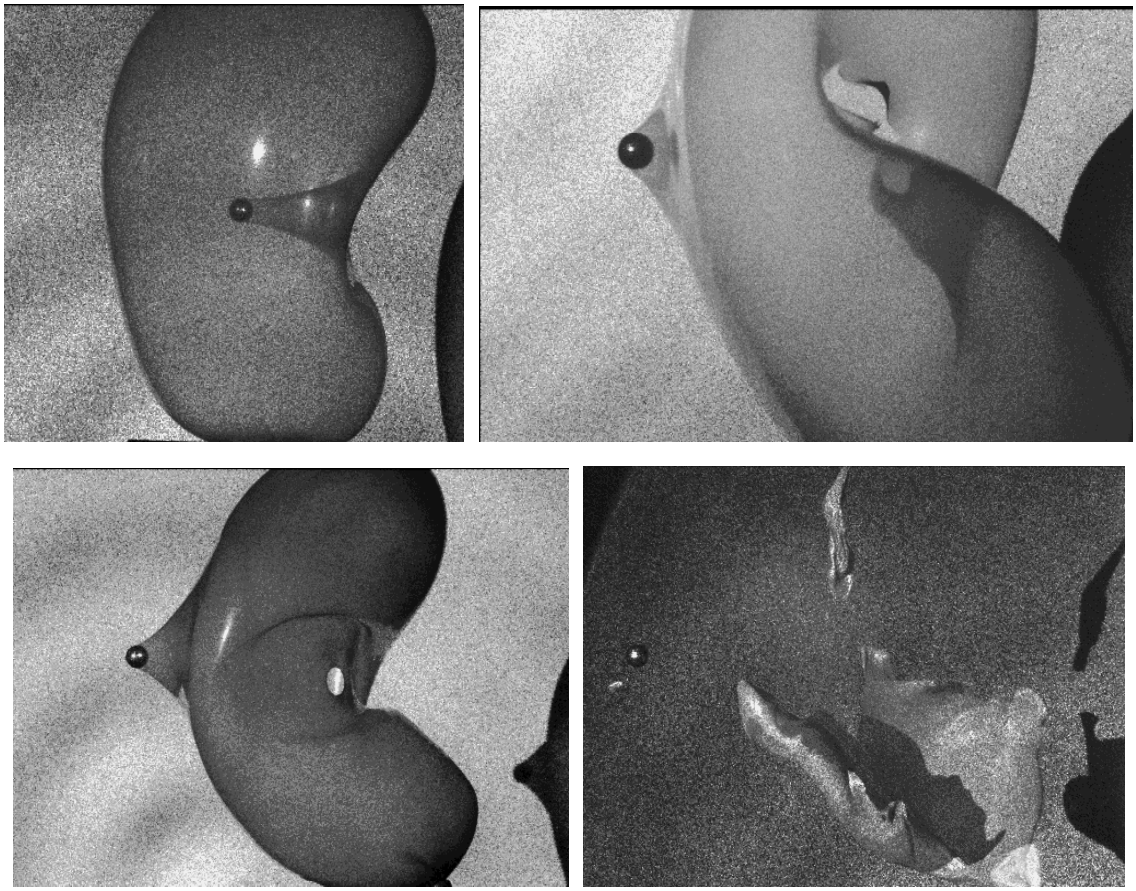

**Figure 2.3.** *High-speed images showing air-gun bullets passing through balloons. The images come from separate shots since only one exposure could be made from each air-gun-shot.*

By measuring the resolution and knowing the velocity and angle relatively to the image plane, the exposure time necessary can be calculated (i.e. how short the exposure time has to be to obtain a sharp looking image). This yields an exposure time of about 1 μs required, meaning that we have not quite used the short pulse length available, but the pictures could not have been taken with an ordinary photographic technique; the use of special electronic flash tubes, sparks or flash bombs alternatively extremely fast shutters, as the Kerr cell shutter, would have been required. Of course the velocity of the bursting balloon could be higher than the bullet-speed at some point, but the velocity of the balloon is not measurable with this set-up. This would mean that the exposure time has to be shorter than the value given above to obtain a sharp image of the balloon fragments.

## 2.3 Discussion

This demonstration was intended to show how high-speed photography using a rather simple technique can make things that are normally concealed to the human eye visible. The pictures shown in this chapter could easily have been taken using a high-speed flash instead of the laser (in fact it might be favourable, allowing colour images) and an ordinary camera. The triggering could be done using a microphone at an appropriate distance from the air-gun (providing the right delay!) to trigger the flash. Thus the technique and equipment required is available to the hobby high-speed photographer [4,5]. The advantage of using a laser is the short pulse length (not really used here, since the velocity of the air-gun bullets was not high enough) combined with the high

intensity. For some applications the monochromicity can be a desirable property, for example when imaging some self-luminous objects. The technique described here should be appropriate for most ordinary high-speed photography applications.

There are, however, applications when visible light can not be used. One example is when a bullet moves inside an opaque material, as illustrated in chapter 3. There are many other applications when the event is simply invisible at optical wavelengths, but can be seen using e.g. X-rays. In the next chapter a high-speed X-ray source is described, and some special properties of this kind of radiation source are discussed together with an example of high-speed radiography using laser-produced X-rays.

*The interested reader can find more information on amateur high-speed photography on the web. At* http://www.rit.edu/~andpph/ *there are a number of different sides of high-speed photography, from a row of articles, to the gallery showing some fascinating images. Many other pages are available (see [1,4,5]), presenting the techniques behind high-speed photography, or stunning images.*

# 3. Generating Ultra-short X-ray Pulses From a Laser Produced Plasma

The principle behind the Laser Produced Plasma (LPP) X-ray source is that a powerful laser pulse, when focused onto a solid target, creates a plasma that emits radiation of many different wavelengths, among them X-rays up to the hard X-ray regime. A short laser pulse results in a short-lived plasma, emitting radiation for only a short while. In our case a laser pulse length of about 100 fs is used, and the resulting X-ray "flashes" have a duration of the order of 1 ps. This means that, considering the opportunities for high-speed radiography, very high-speeds and high resolutions would be allowed without a blurry result. The resolution in our case is, however, as seen later on, limited by the rather low amount of X-ray photons in each pulse. In this chapter the X-ray source is described, first the theory behind the laser produced X-rays, then continuing with the experimental set-up and general properties of the radiation and finally an example of how X-rays can be used in high-speed imaging when imaging a fast event occurring inside a material opaque at visible wavelengths.

## 3.1 Theory

When focusing an ultra-short pulse from a short-pulse high-power laser onto a solid target, a short-lived localised plasma is formed. These plasmas are characterised by their high ion and electron densities and extremely high temperatures, as well as the emission of high-energy X-rays and generation of magnetic fields as high as 100 Tesla. The basic theories behind the laser produced plasmas (LPP) will be presented here in order to provide an intuitive understanding of how the ultra-short X-ray pulses are created.

### 3.1.1 Collective Effects

The plasma is matter in a state of ionisation, either complete or partial. The Coulomb forces between the charged particles in the plasma are relatively strong and long-ranged compared to the interactions of the neutral particles of a gas, therefore each particle in the plasma interacts with a vast number of other particles. When perturbed, the particles tend to respond collectively, due to these strong interactions, giving rise to so called collective effects. In a plasma these collective phenomena are dominant, giving the plasma some rather special properties. Plasma is therefore often called the fourth state of matter [ 9].

An example of a collective effect is the plasma oscillations, i.e. when a collective motion of the electrons relative to the ions is superimposed on the random motion of particles. The angular frequency of the resulting collective electron oscillations is called the *plasma frequency*, $\omega_p$, and is given by:

$$\omega_p = \left( \frac{n_e e^2}{m_e \varepsilon_0} \right)^{1/2} \approx 56.4 \cdot n_e^{1/2}, \qquad \textbf{Eq 3.1}$$

where $\varepsilon_0$ is the permittivity of free space, $n_e$ is the electron density, $e$ the charge and $m_e$ the mass of the electron. There are also other resonant-type phenomena, each with their own typical frequency, as the corresponding ionic collective oscillation - with a characteristic angular frequency obtained simply by replacing $m_e$ with the ionic mass in

the formula above. The presence of a magnetic field gives rise to cyclotron frequencies describing the circular motion of the charged particles.

The response of the plasma to incoming radiation is strongly dependant of these natural frequencies. If the electromagnetic wave has a frequency matching a characteristic frequency, or a combination of them, resonant interaction may take place, giving rise to enhanced energy transfer to the plasma. Considering only the plasma frequency, the dispersion relation for an electromagnetic wave in the plasma is given by

$$\omega^2 = \omega_p^2 + c^2 k^2 .$$

**Eq 3.2**

For $\omega > \omega_p$ $k$ is real, and the wave is transmitted, but for $\omega < \omega_p$ the wave is evanescent (imaginary $k$). Reflection of the wave occurs at the critical density, $n_c$, where $\omega = \omega_p$. This is also the region where the plasma absorbs the most radiation through excitation of plasma waves.

### 3.1.2 Absorption processes

At low laser intensities inverse Bremsstrahlung is the dominant absorption process. Inverse Bremsstrahlung can occur during electron-ion collisions, and the essential effect of this process is that the energy of an incoming photon is converted to kinetic energy of the electron. At higher intensities this process is not that significant, due to the fact that hot plasmas are practically collisionless. When a plasma is created through laser illumination of a solid target, the plasma expands into the surrounding vacuum, creating a density gradient. At the density where the plasma frequency matches the incoming frequency (the critical density) the laser light is absorbed. In the high-intensity region the lower collision frequency reduces the damping of plasma waves and the conditions for their excitation are improved. Two different modes of excitation exist, resonance absorption (also called linear absorption) and nonlinear parametric absorption [ 10].

The plasma expansion proceeds at the local speed of sound, generally about 0.1 nm/fs (100 000 m/s). Since the typical optical skin depth is about 10 nm, laser energy will generally be absorbed in the solid if the laser pulse duration is of the order of 100 fs or shorter [11]. This means that no considerable expansion takes place during the laser pulse. Such a plasma emits X-ray radiation on a time-scale comparable to the laser pulse-length, due to the rapid cooling of a near-solid-density plasma. This rapid cooling occurs as a result of three characteristic properties of this type of plasma: the steep density gradients, allowing fast expansion in front of the target surface; the high thermal gradient, allowing rapid conduction of electron energy to the solid beyond the optical skin depth; and the nonequilibrium conditions in the underionised plasma, allowing the hot electrons to cool rapidly through inelastic collisions with atoms and ions.

When using a laser with a prepulse, a preplasma is created, and the electron density and temperature gradients will not become as steep as in the previous case. This preplasma acts like a shield, preventing the radiation from reaching the solid.

The X-rays from a laser-produced plasma are generally emitted as Bremsstrahlung, as fast electrons are slowed down, and from photodeexcitation and recombination of electrons in the plasma or in the surrounding bulk material.

## 3.2 Experimental Set-up

The generation of X-rays was accomplished by focusing the pulses from a table-top-terawatt laser system ($T^3$-system) into a solid target in a vacuum chamber. The set-up is briefly described in the following sections.

### 3.2.1 The laser system

The X-ray experiments described in this work were all carried out at the Lund High-Power Laser Facility [13]. The laser system is based on the chirped-pulse amplification technique (CPA), using gratings for the stretching and recompression of the pulses. This technique is used in order to reduce the maximum peak power to avoid optical damage in the amplifying crystal and other optical components in the amplifier. This is accomplished through stretching the laser pulse in time before the amplification, and recompressing it after the amplification. The optical layout of the laser system is shown in Figure 3.1

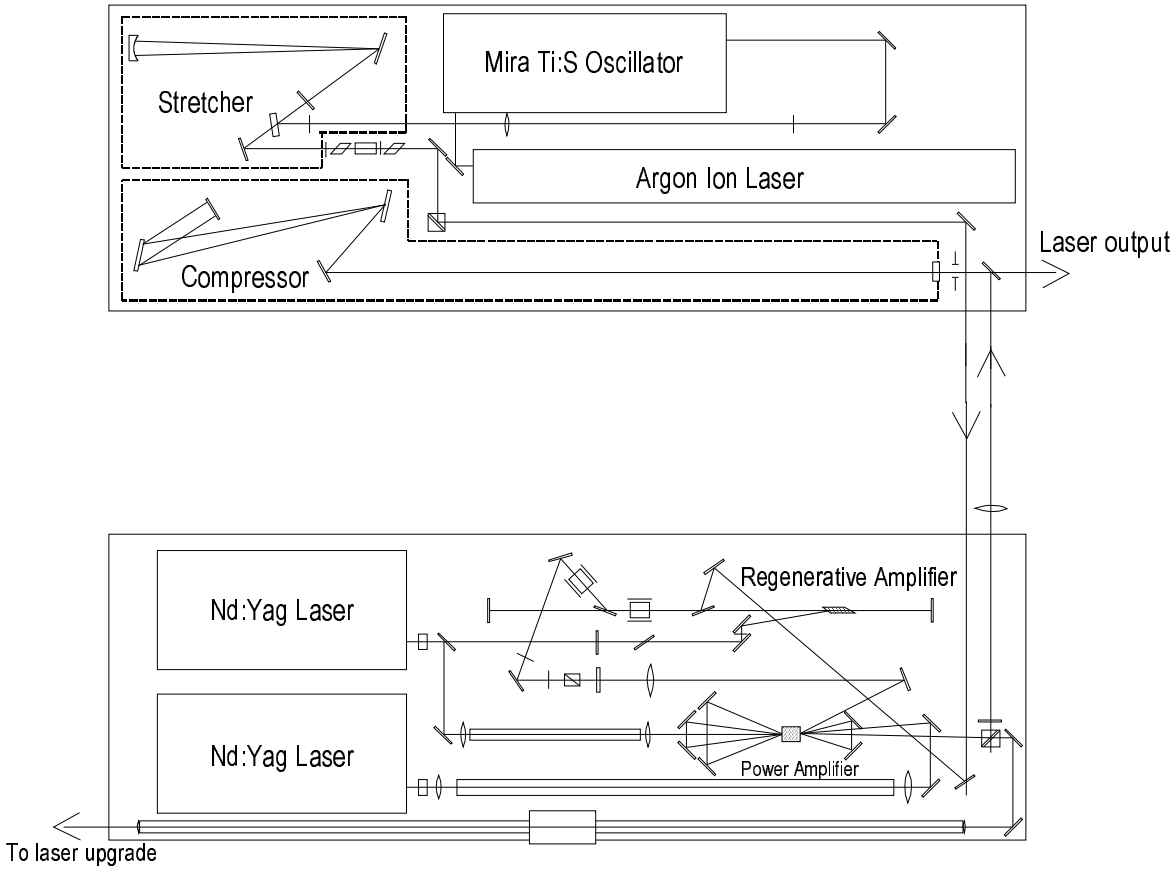


**Figure 3.1** *The Table-Top Terawatt Laser System ($T^3$-system) in Lund. (Supplied by Anders Persson, modified)*

An $Ar^+$-ion laser is used to pump a mode locked Ti:S oscillator generating pulses with a duration of about 100 fs and a repetition rate of 76 MHz. These pulses are stretched in

time by a factor of about 2500 in a grating and mirror arrangement before being injected into a regenerative Ti:S amplifier. There the pulses are amplified $10^7$ times in 15 double passes before ejection through polarisation switching. The final amplification occurs in a four-pass butterfly Ti:S arrangement, where the pulses reach an energy level of up to 450 mJ. Before the recompression the pulse-diameter is increased to approximately 50 mm to avoid optical damage when the pulse-length is decreased again (and subsequently the maximum power increased). The final pulses have a duration of about 100 fs, energy up to 200 mJ and 10 Hz repetition rate at a wavelength of 794 nm (at normal operation). The pulse length of about 100 fs corresponds to a spatial length of about 30 μm, so the laser pulses can actually be seen as thin sheets of light moving through space. The laser system is not possible to trigger externally, but can, of course, be operated in single shot mode.

### 3.2.2 Experimental Chamber

The generation of hard X-rays by focusing a laser beam to high intensities ($>10^{17}$ W/cm$^2$) onto a solid target must take place in vacuum in order to avoid electrical breakdown before the target. A target chamber made of 30 mm thick aluminium with 20 mm thick bottom and top lids (described by Carl Tillman in [14]) was used. An off-axis parabolic mirror with a focal length of 50 mm was used to focus the laser beam onto the target. In order to prevent the focusing mirror from being damaged from sputtering particles, a thin glass plate was mounted in front of the target surface. A thin tantalum (Ta) foil, mounted on a steel disc, was used as target material, and was rotated and moved so that the laser pulses always hit a fresh surface. The rotating target was stabilised with a computer controlled piezo-electric translator, so that the target position relative to the focusing mirror varied with a standard deviation of only 1.5 μm [15]. The chamber was shielded with 5 cm thick lead bricks as protection for the operator. The chamber is also equipped with a steel tube, with windows for the X-ray radiation, that can be lowered into the vacuum-pumped chamber keeping the sample at air-pressure. This tube allows small objects to be placed close to the X-ray source, allowing magnification X-ray imaging.

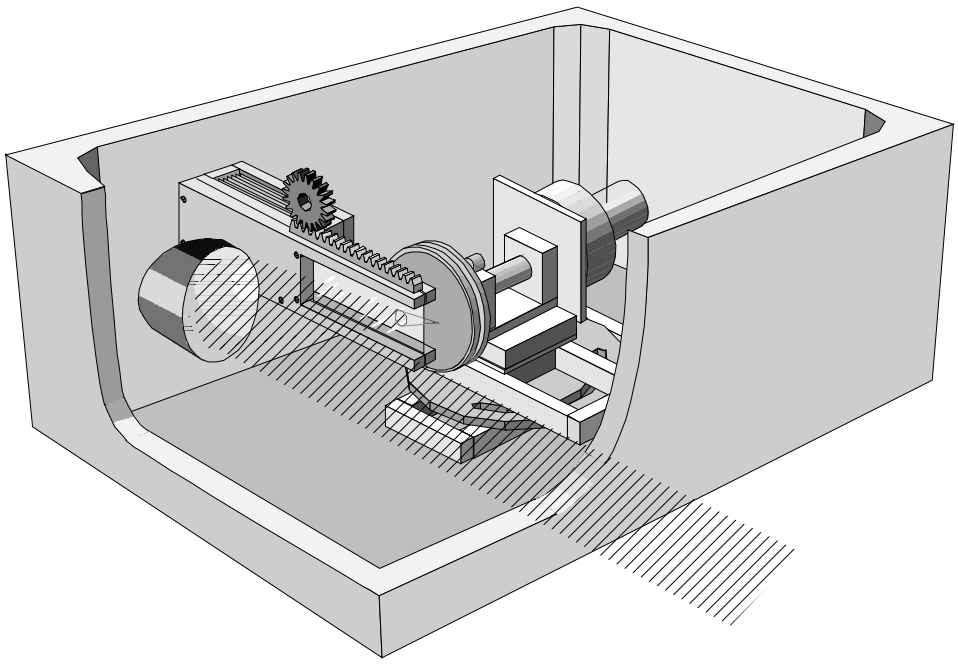

**Figure 3.2** *The target chamber [18]*

### 3.2.3 The X-ray imaging system

The X-ray imaging was performed using image-plates (Fuji BAS 2000), with several advantages compared to conventional X-ray film [ 16].

- The sensitivity is greater by more than 1 order of magnitude
- The dynamic range is $10^4$-$10^5$, compared to $10^2$ for films
- They have linear response to X-ray dose over the entire dynamic range
- They can be reused (and the accumulated background can be erased before use)

The plates consist of a 150-300 μm thick photostimulate phosphor coating of barium fluorohalide crystals, with a trace amount of bivalent europium as luminescence centre ($BaFX:Eu^{2+}$, where the X stands for Cl, Br or I), on a support film made of polyester. When exposed to X-ray radiation, part of the $Eu^{2+}$-ions become $Eu^{3+}$-ions through excitation, releasing electrons to the conduction band. These electrons are trapped in lattice defects, forming metastable colour centres. The exposed plates are scanned with a HeNe laser (633 nm) for read-out, releasing the electrons from the colour centres once again to the conduction band, where they become an excitation state of $Eu^{2+}$, releasing photo-stimulated luminescence (PSL). This light is collected in a photomultiplier tube. The image is stored as a computer file, simplifying image processing and analysis.
The stored pixel value Q of the computer image is given by the formula

$$Q = N\left[\frac{\log\left(\frac{I * S}{const.}\right)}{L} + \frac{1}{2}\right],$$

**Eq 3.3**

where $N$ is the number of grey scale levels, $I$ is the measured value of luminescence light, $S$ is a sensitivity parameter and $L$ is a dynamic range parameter. The parameters $N$, $S$ and $L$ can be set to appropriate values when scanning the images. As default the values $N = 10$, $S = 10000$ and $L = 4$ were used.

To protect the image plates from visible radiation and stress from the surrounding world, they were kept in a special cassette during the exposures. This cassette included an aluminium filter, 1 mm thick, to block out the visible light and soft X-rays. The cassette was placed behind a shield of lead, only exposing a part of the plate at a time, allowing several exposures to be made on each plate before scanning. This was especially suitable because of the relatively small objects, and the fact that there only were two image plates available. Now up to 12 exposures were made on each plate, saving an enormous amount of time and money.

When using the air-gun system (see section 3.4), a CCD-unit was used for imaging using the visible light that also is emitted from the plasma. This unit was placed above the

sample, aimed downwards in order to see where the bullet was (the uncertainty was rather large) to be able to adjust the delay times accordingly. This allowed two images to be made of each shot, from different angles and using different parts of the radiation spectra.

## 3.3 General Properties of the Emitted Radiation

The laser produced X-rays have some interesting properties that are more or less unique to this kind of radiation. The spectrum, as shown in Figure 3.3 reaches all the way up to over 200 keV. The spectrum could also be changed slightly by changing target material, but this possibility was not used in this work, tantalum targets were used all the time.

The X-ray source itself is characterised by its small dimension, measured to be varying between 30 and 100 μm [17], and can in most applications be considered as a point source, emitting uniformly in a large region in front of the target. This allows magnification radiography simply by projecting the object onto the image plate. This comes in handy especially when imaging small objects, and can easily be done in the target chamber used in these experiments. Magnification radiography will be discussed more thoroughly in chapter 4.

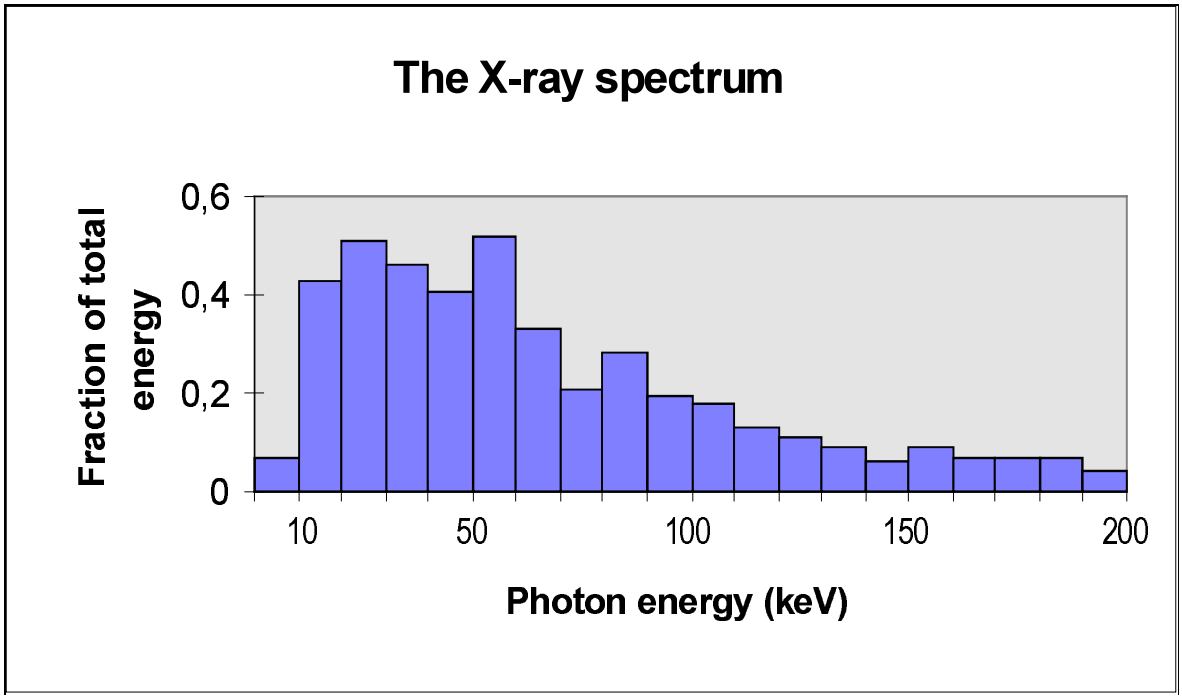


**Figure 3.3** *The X-ray energy distribution from the laser based X-ray source. [ 18]*

The incoming laser pulses have a duration of about 100 fs. The resulting plasma in the target cools off rather quickly, as discussed in the theory section, and the X-ray emission lasts for about 1 ps. These short X-ray bursts with high intensity are suitable not only for high-speed radiography, but also for other applications, as time-gated viewing [ 15].

## 3.4 An example of high-speed radiography using laser-produced X-rays

The ultra-short X-ray bursts that are described in the previous section are most suitable for high-speed radiography when the object or event is moving really fast or when magnification radiography is desired. In this section, however, the event could have been imaged using a less sophisticated X-ray source with significantly longer pulses, such as a high-speed X-ray tube. The event in this case is an air-gun bullet passing through an object opaque at visible wavelengths.

### 3.4.1 Experimental Set-up

The X-ray source is described, in section 3.2. The air-gun system, however, needs some new technical solutions, especially when it comes to the synchronisation of the laser pulse generating the X-rays, and the air-gun shot. Since the TW-laser system is not externally triggerable, a firing system was designed for the air-gun instead, so that the gun could be fired on a given electromagnetic signal. The signal from the shutter-control unit of the laser system, arriving approximately 40 ms before the laser-pulse, was used. The set-up is shown below.

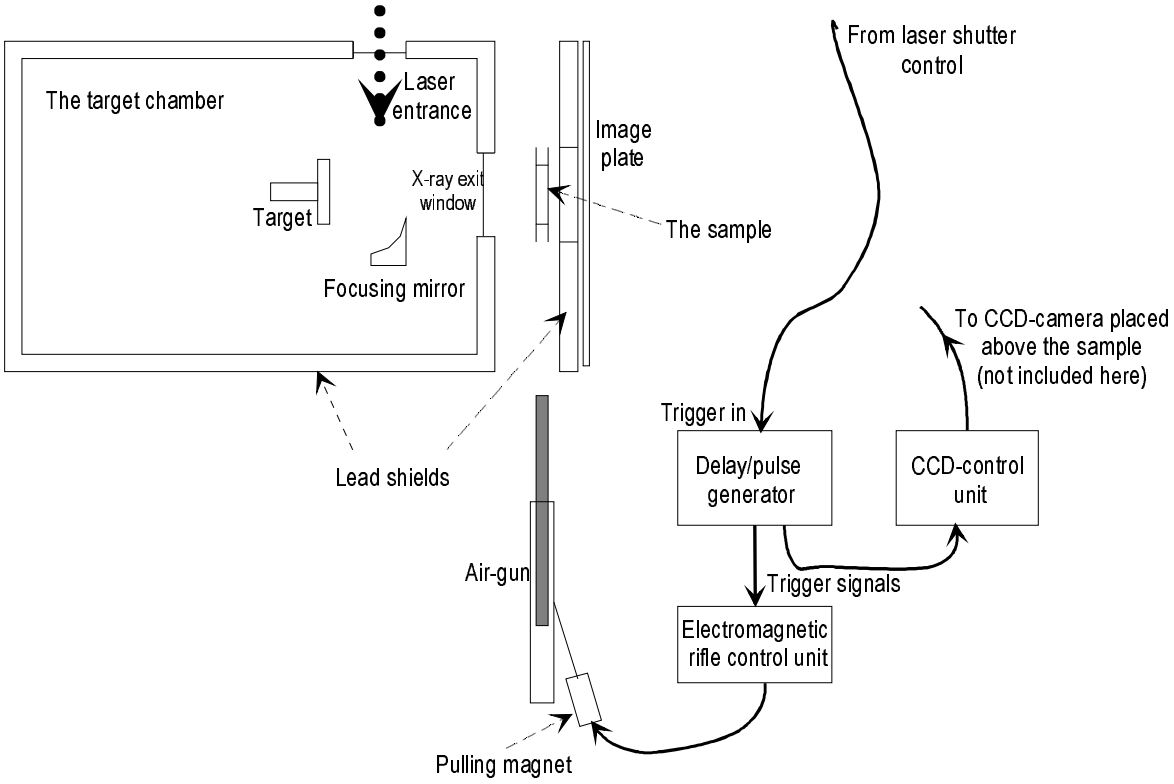


**Figure 3.4.** *The set-up for high-speed radiography of air-gun bullets passing through a phantom*

When the single-shot button is pressed on the laser remote control this shutter-control unit waits for the next laser pulse before opening the shutter, at an adjustable time before the next pulse (in our case about 40 ms). The unit was connected to a Stanford delay/pulse generator which generated the required signals to trigger the CCD-camera and the air-gun triggering unit. On receiving the TTL-pulse from the delay unit, the air-gun triggering unit generated an 18 V pulse (3 A), which was connected to the magnet that pulled the air-gun trigger. The trigger was already pulled part of the distance to decrease the amount of work for the pulling magnet. The uncertainty of the time of the

shot was of the order 1 ms (corresponding to about 14 cm at the speed 135 m/s), small enough to have a pretty good chance of catching the bullet in flight with the X-ray pulse. This uncertainty was probably caused by mechanical imperfections in the air-gun and in the connection between the trigger and the magnet core. An example of an image taken using this set-up is shown in Figure 3.5.

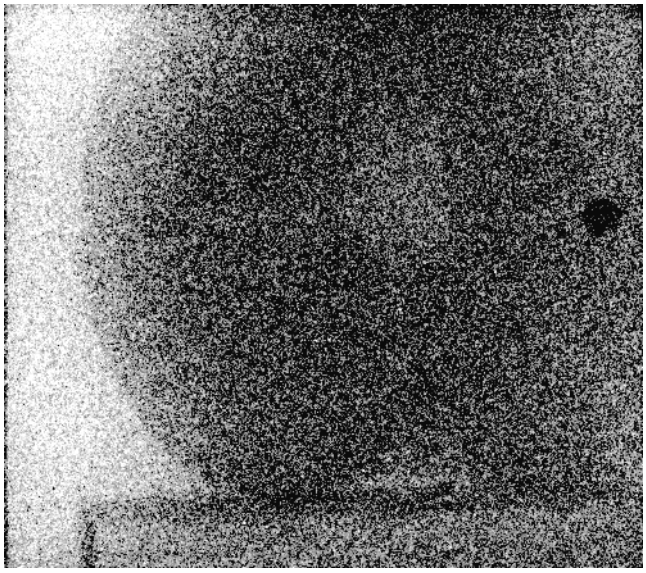

**Figure 3.5** *An air-gun bullet passing through a slice of an apple. The trace of the bullet can only be seen with a little determination and imagination. (The bullet moves from left to right.)*

This image shows that the principle works, but the imaging technique has to be improved. It is very difficult to see that the bullet in fact is moving. The trace of the bullet is virtually invisible.

### 3.4.2 Constructing a phantom

With the triggering problem solved a suitable phantom had to be found to make the images more interesting, not only showing a dark spot representing the bullet in an otherwise uniformly bright surrounding.

#### 3.4.2.1 The substance

The main substance of the phantom had to fulfil the following demands, first of all it was desired that the bullet should leave a trace visible in the X-ray and secondly the possibility to add a contrast agent was wanted in order to be able to improve the contrast. Ordinary butter turned out to be a suitable substance, the consistency can be changed simply by changing the temperature. It also turned out to be fairly easy to add contrast agents as tindioxide ($SnO_2$) and bariumoxide (BaO). BaO, however, was easier to distribute evenly, so the most images were made using BaO as contrast agent.

#### 3.4.2.2 Absorption theory

Having chosen the main substance of the phantom and the contrast agent to use, the contrast agent had to be added in an appropriate amount in order to get the right absorption of X-rays. Since the spectrum of the X-ray source is known (see section 3.3) one can, using the absorption coefficients of the involved materials, calculate the right amount of contrast agent to be added in order to reach the desired absorption. The absorption spectrum of BaO is shown in the figure below.

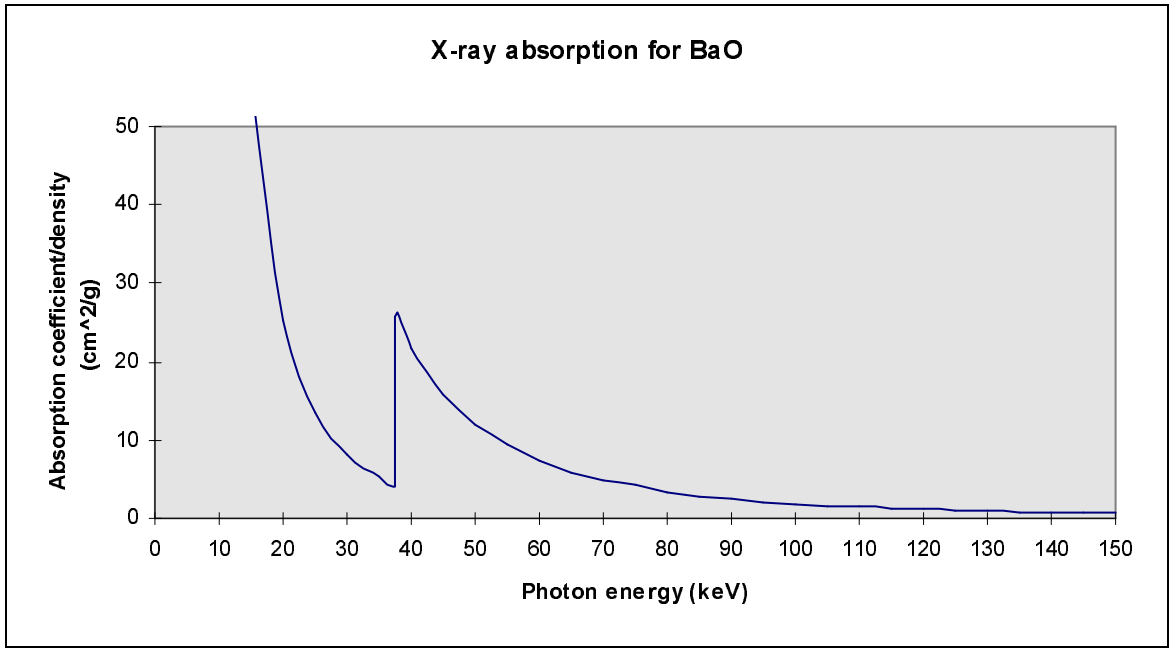


**Figure 3.6** *The X-ray absorption for BaO, given as* $\mu(E)/\rho$ *(*$cm^2/g$*). The Ba K-absorption edge at 37.44 keV is the dominant feature in this part of the spectrum.*

Some test shots were made through a sample of the phantom in order to find out what dimensions that could be expected for the track of the bullet. In a soft sample the track was about 1 cm in diameter (compared with the 4.4 mm diameter of the bullet), so the samples were constructed with a thickness of 15 mm thereafter. This means that the sample-thickness the X-rays pass through varies from about 5 mm in the widest part of the track to about 15 mm in the undisturbed parts of the phantom. With such big difference in thickness, one might ask why the contrast agent is at all necessary. However, without the contrast agent, the sample would not absorb much radiation at all, making the track very difficult to see. On the other hand, if too much of the contrast agent is added, too little radiation would pass through the phantom, again making the track difficult to see. The absorption of X-rays in a material is described by

$$I = I_0 \cdot e^{-\mu(\lambda) l}$$

**Eq 3.4**

where $\mu(\lambda)$ is the absorption coefficient (wavelength dependant) and $l$ the distance the radiation passes through the material. Using this formula for the absorption together with the absorption coefficients (collected at the database at National Nuclear Data Center (NNDC) in Brookhaven [19]) for the phantom and contrast agent, a mix could be found that set the absorption to 50% in the undisturbed part of the phantom. (15 mm thick). This way phantom was constructed where both the hardness and the X-ray absorption could be changed easily when desired.

### 3.4.3 Image enhancement

Using the set-up and phantom described in the previous sections a series of images were made. To suppress the noise in the images some image enhancement was made. The method used is described in [20], and is based on the idea that in each pixel replace the pixel value with the median of the grey scale values of the neighbouring pixels. The

number of pixels to be compared can be set arbitrarily, depending on how much noise has to be suppressed. This method is appropriate in particular when the noise pattern includes spike like components, and where edge sharpness should be preserved. After the noise suppression described, the histograms were modified to improve the visibility of the bullet track. The image enhancement was made in Picture Publisher from Micrografx. In Figure 3.7 below a comparison is made between the original picture, a contrast enhanced picture (only histogram modification) and two pictures enhanced with the median enhancement technique, with different settings, followed by contrast enhancement.

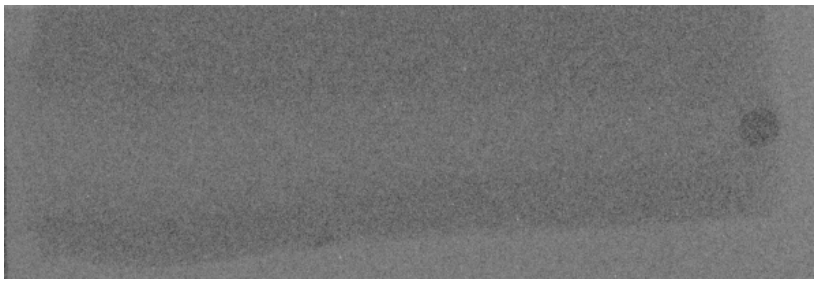

*1. The original image*

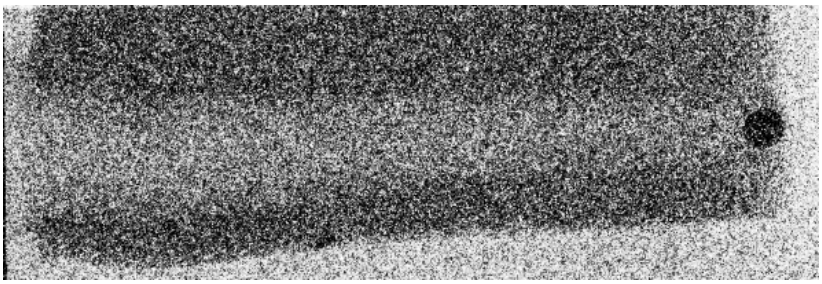

*2. Contrast enhanced image*

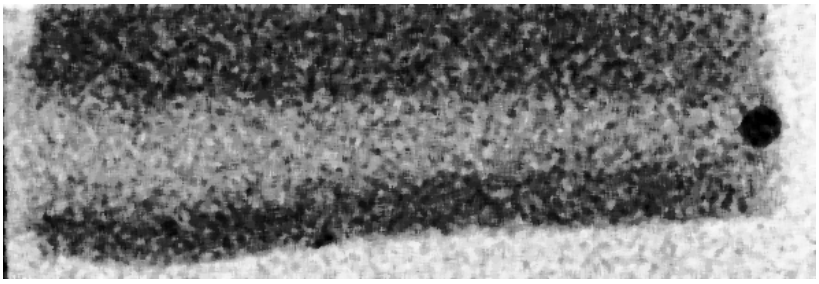

*3. Median filtering (2 pixel surrounding), contrast enhanced*

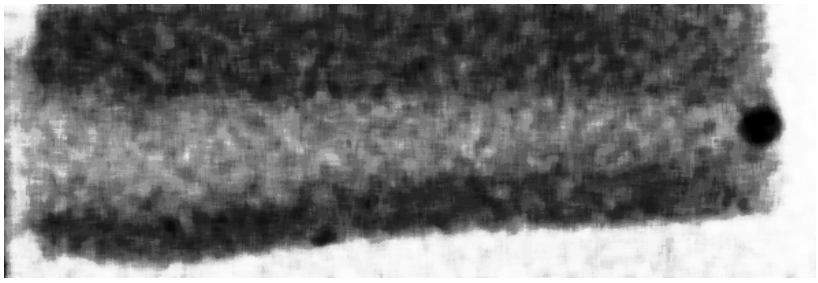

*4. Median filtering (4 pixel), contrast enhanced*

**Figure 3.7** *An illustration the of image processing, as performed on the X-ray images in this work.*

The image enhanced images obviously reveal a lot more about the event than the original picture. In this work all images (except for the first image in Figure 3.7) were contrast enhanced. Most images were median filtered as well, if possible. When the resolution was low from the beginning or when comparisons were made in image quality, median filtering has been avoided.

### 3.4.4 Results

In Figure 3.8 two X-ray images are shown together with the CCD-picture from the same event, both images are made at the same instant in time, showing the event from different angles using different parts of the spectrum. In the CCD-images the bullet is not visible, but the entrance hole is visible, and in a few images the bullet is almost through at the other side, so a small bulge is seen in the other end. In the X-ray image the track is clearly visible. Unfortunately the noise level is rather high in the X-ray images, due to the small number of photons that hit the image plate from one pulse.

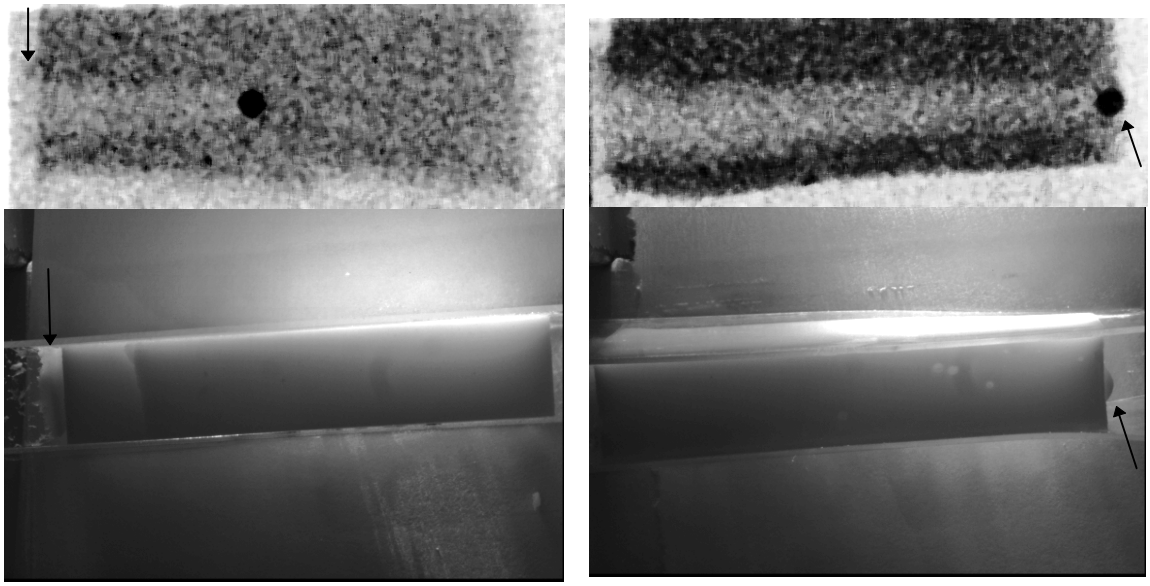

**Figure 3.8** *Two different X-rays images of air-gun bullets passing through the phantom. Below the X-ray image the corresponding picture taken with the CCD-camera is shown. Notice especially the splash at the bullet entrance in the left image pair, and the bulge from the bullet almost through at the other end in the right images.*

The shape of the bullet trace, as seen above, gives information of the speed of the expansion occurring behind the bullet. The bullet velocity is known to be 135 m/s, and assuming that the bullet is not slowed down to any greater extent, the average expansion speed can be estimated to about 10 m/s in the fairly soft phantom. The highest expansion velocity is of course found in front of the bullet, where the speeds are of the same order as the bullet velocity. The final diameter of the trace is about 15 mm.

This was just an example of how high-speed radiography can be put into use investigating phenomena impossible to see using visible illumination. This experiment could, as already mentioned possibly have been carried out using a high-speed X-ray tube. The main problem with the laser X-ray source in this case is the rather high noise level. The noise level decreases proportional to the square root of the number of photons, so a larger amount of photons would result in higher quality of the images. This is discussed more thoroughly in the next chapters.

# 4. Studying laser ablation using radiography with a laser produced X-ray source

An interesting field to study using laser produced X-ray imaging is the deformation of a material when a powerful laser pulse is focused onto its surface. Such an event is very fast and at the same time in itself strongly luminous, so some kind of special technique has to be used. In this chapter laser produced X-rays are put to use so that the emitted radiation can be filtered away easily in front of the image plate. This technique also allows the crater to be imaged in profile, showing the depth and shape of the crater at different times as it grows.

## 4.1 The geometry

The first studies performed here were made without magnification, and show already formed craters, just as a study of what contrast that can be expected and how much that really can be seen in the images. The noise level was, however, far too high to be able to draw any useful conclusions about the laser ablation phenomenon, as can be seen in Figure 4.1.

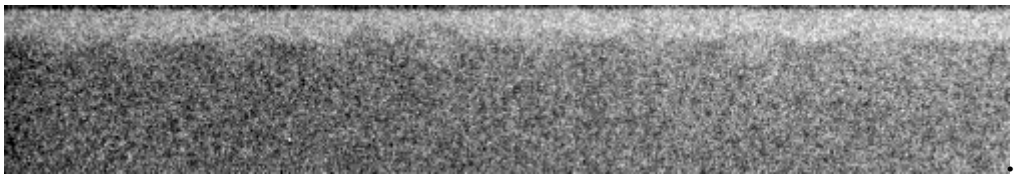

**Figure 4.1** *A row of craters at 1:1 imaging.*

The experiment above clearly shows that the noise level is too high at normal imaging with this set-up. This means that somehow a technique has to be found to reduce the noise. The noise level is proportional to the square root of $N$, where $N$ is the number of photons in this case. Accordingly the noise level would decrease with respect to the signal if the number of photons is increased. The conclusion is that somehow the number of photons passing through the crater has to be increased.

The most obvious way to increase the number of photons is of course to increase the laser intensity, as will be discussed in the next chapter. There is, however, a way to increase the number of photons passing through the sample without changing the laser output; through moving the sample closer to the target. The image plates are difficult to move closer to the target because this would mean that they would have to be placed inside the target vacuum chamber. That would be very inconvenient since the target chamber would have to be opened between every exposure. Keeping the image plates outside the chamber, the sample can be lowered into the chamber using the sample lowering tube, allowing magnification radiography. This geometry would result in a larger amount of photons passing through the sample, but the same number of photons hitting the image plate. Still this is definitely an improvement, since the pixels of the resulting image can be added together. This way the resolution should be equivalent to the one achieved without magnification, but the number of photons in each new “pixel” would be increased by approximately the magnification factor. In Figure 4.2 the geometry for magnification radiography is shown.

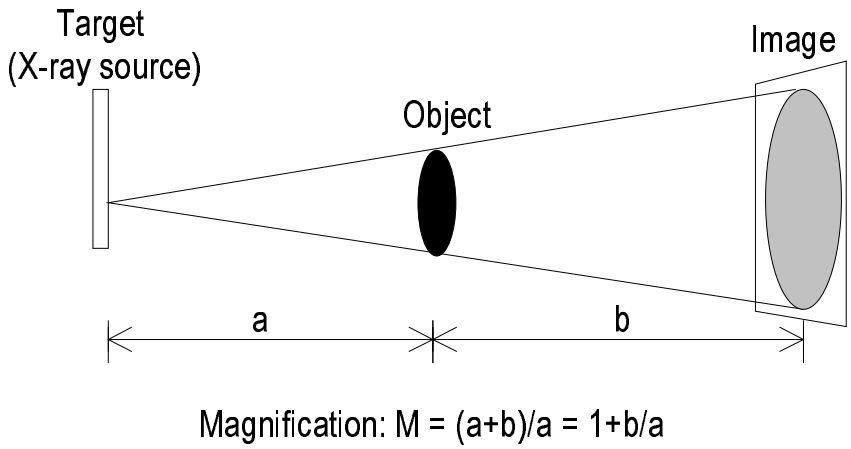


**Figure 4.2.** *The principle behind magnification radiography. The X-ray source can be approximated as a point source when the object is much larger than the source itself.*

This geometry was tested, with the magnification factor equal to 10, once again using static imaging (already formed craters), resulting in the picture shown in Figure 4.3. As can be seen, the contrast has improved greatly from the previous experiment. The most significant change is that the crater shape is much easier to distinguish with good accuracy.

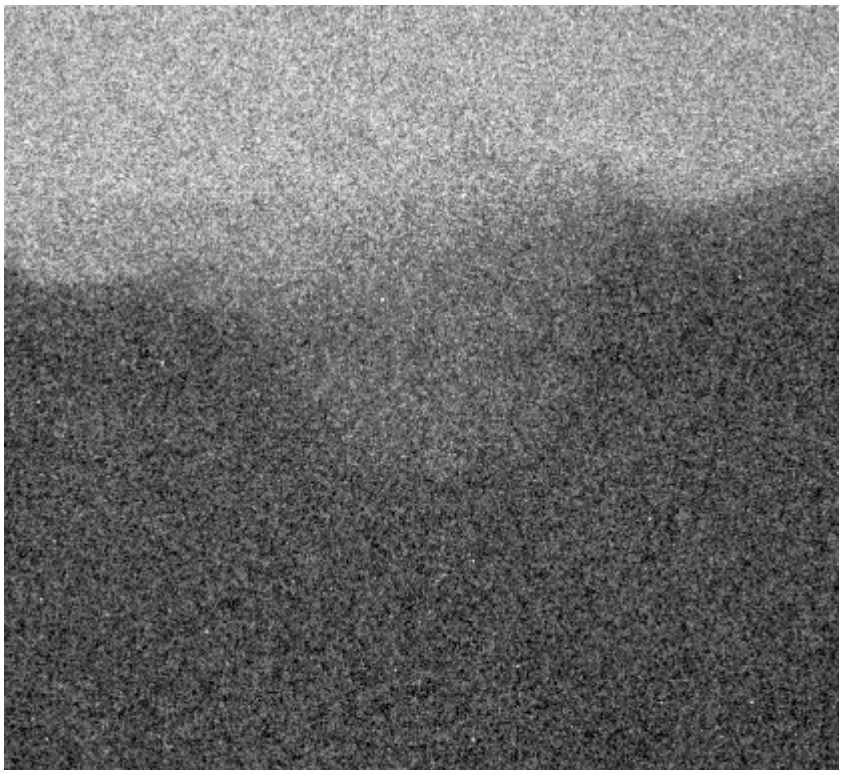

**Figure 4.3** *A crater imaged using ten times magnification.*

It should be pointed out that Figure 4.1 and Figure 4.3 are shown here in the same scale and the crater are of approximately the same size, i.e. the size difference of the crater images only comes from the magnification introduced by projection imaging, according

to Figure 4.2. The crater size was about 5 mm in diameter, and the phantoms were about 7 mm thick. The only image enhancement made is histogram modification, performed in an equivalent manner for both images. As the object size is much larger in the magnified image, it is more suitable for image enhancement as median filtering. Magnification radiography turned out to be such a promising technique that it had to be tested in a real high-speed context, that is, probing the crater forming at different times during and after the laser ablation pulse.

## 4.2 The Experimental Set-up

The X-ray source is described in the previous chapter, but the laser ablation study also requires the use of a second laser. In this experiment an Nd:YAG-laser was used. The laser pulses have a maximum energy of 5 J and a duration of approximately 10 ns FWHM (Full Width at Half Maximum). In these experiments a laser pulse energy of about 1 J was used. The Nd:YAG laser is shown in Figure 4.4.

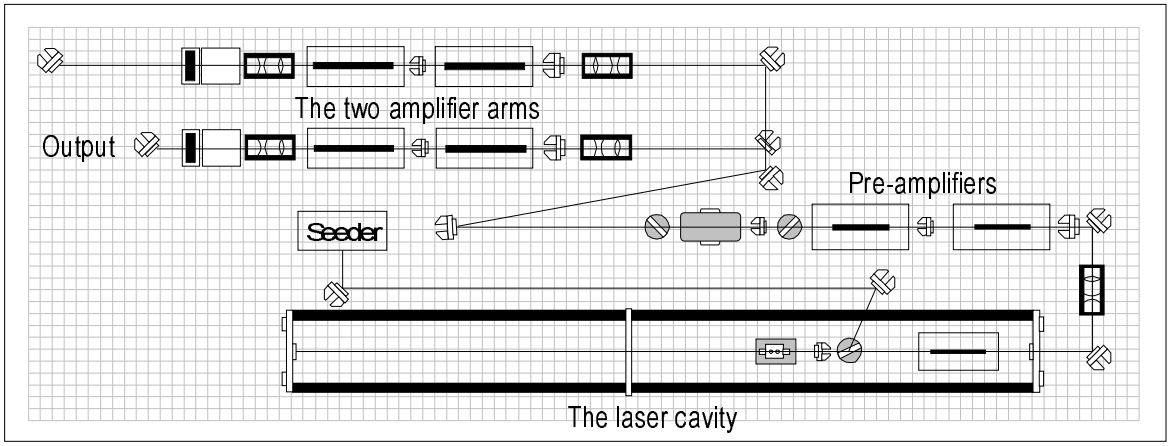


**Figure 4.4** *The Nd:YAG-laser used for the laser ablation study. (Supplied by Anders Persson, modified)*

The laser cavity is seeded by a diode laser. After the cavity the beam is amplified in two steps, then split up in two different amplifier arms each containing two more amplifiers. Only the lower arm in Figure 4.4 was used in this experiment. The Nd:YAG-laser is now used for the $T^3$-laser upgrade that recently has commenced.

The Nd:YAG laser pulses were focused a few centimetres below the sample surface since this arrangement had shown to be most favourable for crater generation in earlier test experiments. The Nd:YAG laser was triggered by the master clock of the TW-laser, both lasers ticking at 10 Hz. The time difference between the laser pulses could be set arbitrarily on a delay/pulse generator (as used in earlier chapters). Through the use of two synchronised shutters one pulse from each laser could be selected, with the previously chosen time difference. Two photodiodes, with risetimes of less than 1 ns, were used to measure the time difference between laser pulses, so it could be determined at what time relatively to the ablation laser pulse the actual imaging was made. The jitter in time differences turned out to be no greater than one nanosecond.

The phantom, where the laser ablation would take place, was equivalent to the one described in the previous chapter. In preceding experiments the laser produced craters

turned out to be about 5 mm in diameter. Accordingly, the sample thickness was set to 7 mm. Knowing the sample thickness and the expected crater size, the amount of contrast agent (BaO) to be added to the phantom could be calculated, as described in section 3.4.2.2.

The sample lowering tube was used for the magnification radiography in order to lower the samples into the target chamber, keeping the samples at air-pressure. Transparent sample holders were constructed, easy to lower into the sample tube, protecting the tube from the splashing phantom when the crater is formed. They also made sure that the samples were placed in the same position each time. A wooden model of the desired shape was built and the sample holders were then fabricated using shrinking plastic that, when heated, shrinks and is formed after the wooden model. In this manner a number of holders were built so that the samples could be exchanged quickly and easily.

## 4.3 Results

With the set-up described above, laser ablation could be imaged successfully on a nanosecond scale, i.e. the imaging moment could be set with nanosecond accuracy. The time between the ablation laser pulse and the X-ray burst was measured using two photo-diodes with rise-times of less than one nanosecond. The resulting images are shown in Figure 4.5, together with the corresponding delay times.

The first image shown in the figure is made when the laser pulse reaches approximately the half maximum, since t = 0 is set to be in the middle of the pulse and the pulse width is approximately 10 ns FWHM, as mentioned earlier. Correspondingly the image at 0 is made in the middle of the pulse, the image at 5 ns where the pulse once again reaches the half maximum value, and the image at 10 ns represents the end of the pulse. All the other pulses shown here are made after the pulse has ended.

## 4.4 Discussion

The images presented in the previous section show that laser ablation can be imaged successfully on a nanosecond scale using X-rays from a laser-produced plasma source. As can be seen, however, the crater forms relatively slowly, no ablation is visible before the 10 μs image, implying that the time-scale was a bit different than expected. No imaging (except for the image showing the final crater form) was made with a greater delay than 10 μs, because on that time-scale there are other, more conventional techniques available for imaging. The sizes of the craters shown in the last two pictures in Figure 4.5 can be estimated using the magnification factor determined earlier to approximately 10. This yields a crater size of 2.1 mm at 10 μs, and a final crater diameter of 4.9 mm. Using the crater at 10 μs, it is possible to give a rough estimation of the velocity of the moving substance. In ten microseconds the substance has moved a distance of the order of 1 mm, corresponding to a velocity of the order of (1 mm)/(10 μs) = 100 m/s, which is of the same magnitude as the previously presented air-gun bullets. This velocity was lower than expected. The maximum velocities in the sample can of course be much higher.

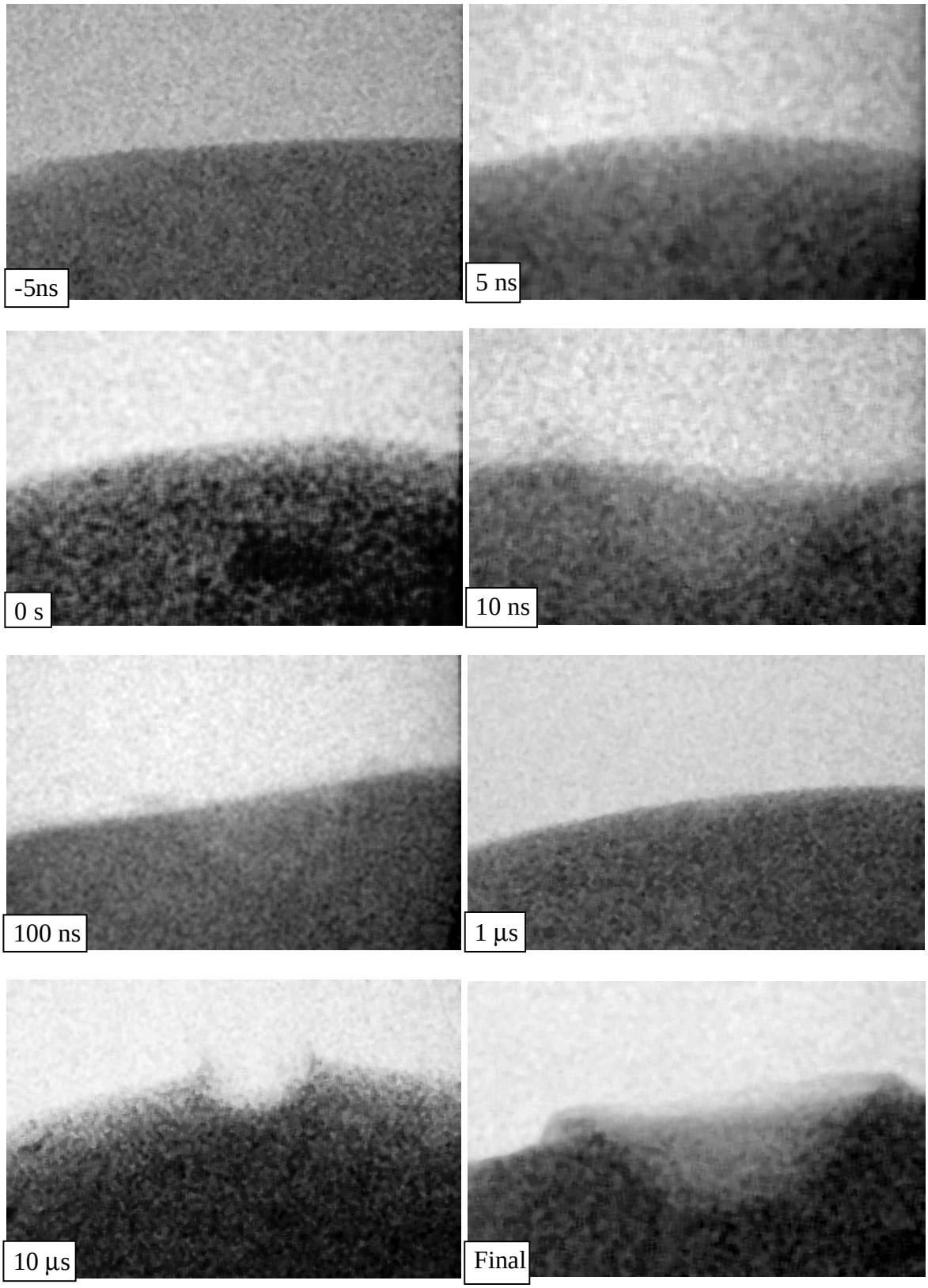


**Figure 4.5** *Laser ablation studied on the nanosecond scale. As can be noticed, the laser intensity and the sample shape varied somewhat from shot to shot. All images are made with ten times magnification.*

The crater-like shapes at 10 ns and 100 ns after the laser ablation pulse is probably only due to variations of the initial shape of the sample and is not actually a crater. Other

images taken in that interval do not show this crater-like phenomenon. There is, however, a slight possibility that it is an actual physical phenomenon, that the X-ray absorption in that area has been affected by the incoming laser pulse, but no such conclusions can be drawn from these images.

## 4.5 Summary

It has here been shown that laser-produced X-rays can be successfully employed for the imaging on a nanosecond scale of a laser ablation event. In this particular substance, however, the ablation takes place on a rather long time-scale, allowing more conventional X-ray generation techniques to be used, e.g. high-speed X-ray-tubes. This imaging method, however, allows investigation nanosecond by nanosecond of how an ablation phenomenon occurs, and the use of magnification radiography also can give a good resolution image of small craters forming.

# 5. Discussion

High-speed radiography using a laser-produced X-ray source is a rather new field, requiring more investigation. Some improvements have to be made before it can be put to more extended use commercially or in research. Here a few improvements are suggested, and also some possible future applications, where high-speed radiography using laser-produced X-rays could become an important tool, are pointed out.

## 5.1 Future Improvements

In order to make high-speed radiography with laser-produced X-rays a more suitable tool for research and commercial use, some improvements are necessary. First of all the X-ray yield is discussed, and then more practical problems.

As can be seen in the images in the previous chapter there is some substantial noise that has to be removed through image processing to make the images useful. The noise-level is high due to the rather small amount of photons in each X-ray pulse. Since the noise-level is proportional to $\sqrt{N}$, and the signal proportional to *N*, where *N* is the number of photons in this case, the noise-level will appear weaker in comparison with the signal when the number of photons is increased. This can be seen clearly in the figure below, where the same row of "craters" is imaged four different times, each with a different number of X-ray pulses. This way one can find out approximately what images taken with more powerful X-ray yield would look like. The object is of course static in these images.

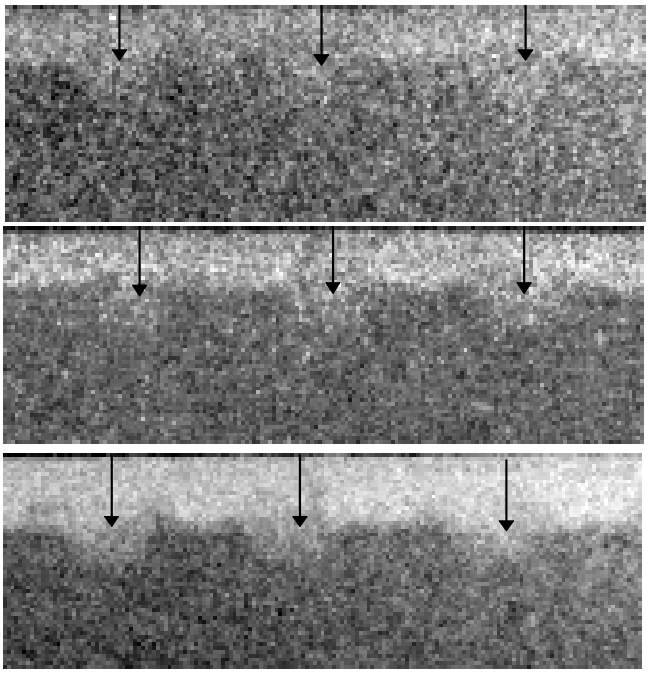

a) The craters imaged with one X-ray pulse (as normal for high-speed imaging)

b) The same craters, with two exposures

c) Five exposures

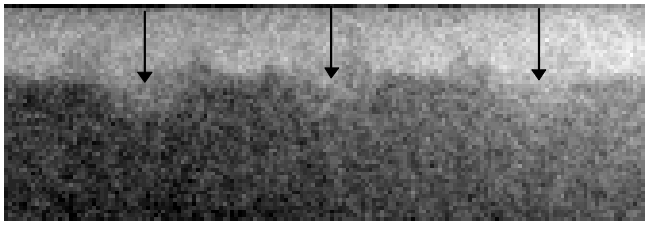

d) Ten exposures

**Figure 5.1** *A row of craters imaged without magnification, with 1, 2, 5 and 10 exposures respectively. This is done to simulate more powerful X-ray sources.*

As mentioned earlier the noise can be reduced through magnification radiography. In Figure 5.2 a magnified crater is shown, to the left exposed with just one pulse, and to the right exposed with four X-ray pulses, and the difference is rather obvious.

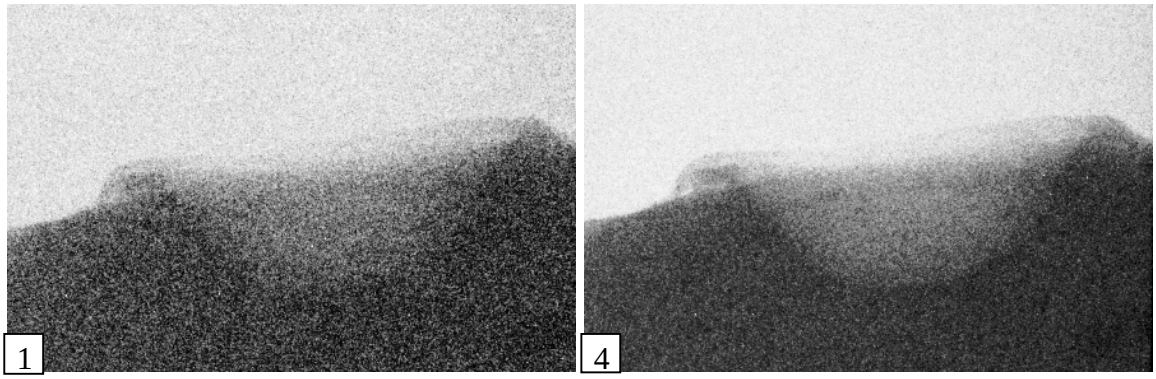


**Figure 5.2** *A crater imaged with one and four exposures respectively. Only enhanced through histogram modification.*

The X-ray yield does not depend linearly on the laser intensity. In [21] the X-ray intensity for energies above 50 keV, using a picosecond TW-laser, is found to depend on the laser intensity accordingly:

$$i_x \propto I_L^{2.8},$$

**Eq 5.1**

where $i_x$ is the X-ray intensity, and $I_L$ the laser intensity. If this would be valid also for shorter laser pulses, as used in this work, it would mean that the laser intensity only has to be 2.3 times the current value to result in ten times as high X-ray intensity. What this would mean for the high-speed radiography is clearly visible in Figures 5.1 and 5.2 above.

An upgrade of the $T^3$-laser used in these experiments has started, and the expected new energy in the upgraded laser pulses is about 750 mJ, still in 100 fs pulses, corresponding to a power of 7.5 TW. The current set-up, as described in section 3.2.1 will also be fully functional, with a slight decrease in maximum power, since the amplified pulses are splitted in two, a part of the beam is redirected to the new amplifying crystal. The Nd:YAG-laser used to generate the craters in the laser-ablation experiment is now employed for the pumping of the upgrade amplifier crystal.

As of today the lasers with capability to generate enough X-rays for high-speed radiography applications are huge and expensive. In addition they are still rather rare, so right now the commercial possibilities of the technique introduced in this work are limited. In the future, however, new generations of lasers will arrive, more compact and cheaper, making them available also for other applications than basic research. The time-scale for this development is not easy to predict, as always when discussing the future. For the development of new lasers it is important to find applications to motivate the continuation of research in this field, to predict the new possibilities new generations of lasers would involve.

## 5.2 Possible Applications

The X-ray pulses from the laser-produced plasma source have some special characteristics; the short pulse length, the small source size and high intensity. These properties is especially suitable for the imaging of small, ultrafast events, where the imaging using visible light is impossible for one reason or the other. The event could be strongly luminous, or could occur inside an opaque material. An example of such an event can be laser ablation, but as seen in this work, the velocities can be rather low in some materials. Laser ablation phenomena that might be interesting to study using this technique can be e.g. in medicine; lasers are often used to remove tumours, and such processes could be interesting to watch on a short time-scale.

High-speed radiography using laser produced X-rays has been shown here successfully to be a suitable tool for the imaging of ultrafast events on the nanosecond scale. The possibility to study laser ablation phenomena on the nanosecond scale can give new information of how the craters are formed.

Another field that can be interesting to study are laser driven shocks in foam materials, as discussed in [22]. The shocked region moves with a velocity of several times the local speed of sound. The compression in this region affects the X-ray absorption, making these shock-waves possible to “see”. This kind of studies is important for the study of inertial confinement fusion.

# 6. Acknowledgements

A number of person have been of great help during these experiments. First of all I would like to thank my supervisor Claes-Göran Wahlström, who has been a great source of ideas and has helped me find solutions to practical problems even at "odd" hours.

Carl Tillman has been of great help in helping me carry through the experiments, as an information source and simply as someone to discuss the problems and successes of this work.

I would like to thank Laurence Kiernan and Matthias Grätz for lending me laser-time now and then, and I hope I have not been to much of a nuisance.

I would like to thank all the other people who have helped me during this work, e.g. Anders Persson for helping me with the lasers, Åke Bergquist for help with electronic equipment, Bertil Hermansson for help with computers (software and hardware), and, and, and...

To be sure I have not forgotten anyone, I would like to thank everyone else at the Division for Atomic Physics in Lund that has helped me during this work. It has been a pleasure working with you all.

# 7. References


1. *Edgerton related links* at http://www.hamilton.net/aurora/city/links9.htm

2. W. Yuren, *Laser High-Speed Photography Systems Used To Ammunition Measures And Tests*, SPIE Vol. 1346 Ultrahigh- and High-Speed Photography, Videography, Photonics, and Velocimetry 1990, pp 331-337.

3. J.E. Field, *High-Speed Photography*, Contemp. Phys., Vol. 24, No. 5, pp. 439-459 (1983)

4. A. Davidhazy, *High Speed Photography*, "http://www.rit.edu/~andpph/text-high-speed.html"

5. L. M. Winters, *High-speed Flash Photography for Amateur Photographers,* "http://www.pacsci.org/public/education/gallery/high_speed_photos/fpaper.html ", "http://www.pacsci.org/public/education/gallery/high_speed_photos/default.html " shows some pictures taken by students.

6. S. V. Yevdokimov, Ye. V. Nilov and A. A. Chertkov, *Application of Lasers For High-Speed Photography of Fast Processes*, Laser and Unconventional Optics Journal, No. 64, pp 12-15 (1976)

7. A. Davidhazy, *Schlieren Photography*, "http://www.rit.edu/~andpph/text-schlieren.html"

8. D. Hoarty, A. Iwase, C. Meyer, J. Edwards, and O. Willi, *Characterization of Laser Driven Shocks in Low Density Foam Targets*, Physical Review Letters, Vol. 78, No. 17, pp. 3322-3325 (1997)

9. P. K. Carroll and E. T. Kennedy, *Laser-Produced Plasmas,* Contemp. Phys., Vol.22, No. 1, pp. 61-96 (1981)

10. E. T. Kennedy, *Plasmas and Intense Laser Light,* Contemp. Phys., Vol. 25, No. 1, pp. 31-58 (1984)

11. M. M. Murnane, H. C. Kapteyn, M. D. Rosen and R. W. Falcone, *Ultrafast X-ray Pulses from Laser-Produced Plasmas*, Science Vol. 251, pp. 531-536 (1991)

12. B. N. Chichkov, C. Momma, A. Tünnermann, S. Meyer, T. Menzel, and B. Wellegehausen, *Hard-x-ray radiation from short-pulse laser-produced plasmas,* Appl. Phys. Lett., Vol. 68, No. 20, pp. 2804-2806, (1996)

13. S. Svanberg, J. Larsson, A. Persson, and C.-G. Wahlström, *Lund High-Power Laser Facility - Systems and First Results*, Physica Scripta, Vol. 49, pp. 187-197, (1994)

14. C. Tillman, *Characterisation and Applications of Hard X-rays from a Laser-Produced Plasma Source*, Licentiate Thesis, LRAP-188, Lund Institute of Technology, Lund, Sweden (1995)

15. M. Grätz, *Hard X-rays from a Laser-Produced Plasma: Source Characterization and Applications*, Licentiate Thesis, LRAP-208, Lund Institute of Technology, Lund, Sweden (1996)

16. J. Miyahara, *The imaging plate: A new radiation image sensor*, Chem. Today, Vol. 223, pp. 29-36 (1989)

17. A. Nykänen, *Spatial Characterisation of a Laser-Produced X-ray Source*, Diploma Paper, LRAP-210, Lund Institute of Technology, Lund, Sweden (1997)

18. C. Tillman, *Development and Characterisation of a Laser-Based Hard X-Ray Source*, Doctoral Thesis, LRAP-204, Lund Institute of Technology, Lund, Sweden (1996)

19. National Nuclear Data Center, Brookhaven, "http://www.nndc.bnl.gov/"

20. R. C. Gonzalez and P. Wintz, *Digital Image Processing*, 2nd ed., Ch 4, pp 144-175 (1987)

21. M. Schnürer, M. P. Kalashnikov, P. V. Nickles, Th. Schlegel, W. Sandner, N. Demchenko, R. Nolte, and P. Ambrosi, *Hard x-ray emission from intense short pulse laser plasmas*, Phys. Plasmas, Vol. 2, No. 8 (1995)

22. B.A Hammel, D. Griswold, O.L. Landen, T.S. Perry, B.A. Remington, P.L. Miller, T.A. Peyser, and J.D. Kilkenny, *X-ray radiographic measurements of radiation-driven shock and interface motion in solid density material*, Phys. Fluids B, Vol. 5, No. 7, pp. 2259-2264 (1993)